14th Australasian Fluid Mechanics Conference
Adelaide University, Adelaide, Australia
10-14 December 2001

Damping of internal gravity waves in stratified fluids

G. O. Hughes

Research School of Earth Sciences
The Australian National University, Canberra, ACT 0200, AUSTRALIA

Abstract

I present a combined experimental and theoretical investigation of damped internal gravity waves in a stratified fluid. Three parameters determine the flow behaviour — the excitation frequency of the wavefield, the flow aspect ratio, and a Reynolds number based on the strength of the stratification and the flow depth. Damping is found to be very significant for internal gravity waves of low frequency (up to at least $0.01N$, where N is the buoyancy frequency) over a wide range of flow aspect ratios and Reynolds numbers.

A theory that incorporates spatially uniform damping of internal waves is compared with measurements. This theory provides a significantly better description of the wavefield than is possible with traditional theory, which neglects damping.

Introduction

In stratified environments such as the atmosphere and oceans, numerous mechanisms exist that locally disturb surfaces of constant density from their equilibrium position. As buoyancy forces seek to restore the local equilibrium, internal gravity waves are commonly radiated away from the disturbed region. These waves transport both energy and momentum vertically, and as such, represent a very important process by which motion at different levels in a stratified flow can be coupled.

In most geophysical flows the internal wavefield is subject to damping by the stresses arising from background turbulence. LeBlond [1] first considered theoretically the damping of internal waves in a turbulent fluid. He found that the evolution of shorter wavelength waves are influenced most by such damping.

In this study I use a novel experiment to examine the damped wavefield. Wong, Griffiths & Hughes [3] showed that vertical motion of the wave source relative to the ambient fluid selects a dominant internal wave mode. Here the wavefield is maintained in a steady-state in the laboratory frame of reference by the uniform vertical advection of ambient fluid past a time-invariant forcing. I examine the damping characteristics of a range of internal wave modes by varying the rate of vertical advection. This set-up is closely related to an oscillatory forcing in a frame of reference fixed with respect to the fluid. Measurements of the wavefield are compared with inviscid theory and with a theory incorporating viscous damping.

Experiments

In all experiments, the tank shown in Figure 1 was linearly stratified with salt to a depth of approximately 30 cm using the 'double-bucket' method. The buoyancy frequency $N = (-g/\rho_0 d\rho/dz)^{1/2}$ was chosen to be either 0.4 or 1.3 rad s^{-1}. Here, $d\rho/dz$ is the background vertical density gradient, g is the gravitational acceleration and ρ_0 is a reference density.

The internal wavefield was excited in these experiments by the continued addition of fluid from the double-bucket system into the float at the top of the stratification. The base of the float was a porous sponge, through which buoyant input fluid percolated with zero vertical momentum. Thus the internal wave excitation consisted of a steady stress at the free surface due to the horizontal outflow from the float.

Fluid was introduced at the top of the tank at several different flow rates. Meanwhile the valve at the tank base was opened to allow fluid to drain through the permeable boundary. For each input flow rate the valve was adjusted so that the tank depth was held constant. The head loss of the flow through the permeable boundary was large compared with that in the remainder of the flow. Vertical advection of fluid in the tank was therefore spatially uniform.

Three dimensionless parameters govern the behaviour in this experiment:

(i) the dimensionless vertical advection speed $w_a{}' = w_a/NH$,

(ii) the Reynolds number $Re = NH^2/\nu$, and

(iii) the flow aspect ratio $L' = H/L$.

Primes are used here to denote dimensionless quantities; w_a is the velocity at which fluid is advected vertically, H is the tank depth, L is the tank length and ν is the fluid viscosity. In these experiments $L' = 0.25$, $w_a{}'$ was varied between 1×10^{-5} and 3×10^{-4}, and Re took values of either 3.5×10^4 or 11.5×10^4.

The horizontal velocity profile in the tank was visualised by releasing a series of vertical dye lines from the centre of the tank. A video record of the experiment was used subsequently to determine the vertical wavelength, the wave amplitude and the rate of attenuation of wave motion with height. I present only measurements of the vertical wavelength in this paper.

Internal waves are excited in this experiment by steady forcing in a frame of reference fixed with the tank. These waves have vertical wavelength $\lambda = 2\pi/m$, where m is the vertical wavenumber. The equations describing the transformation between frames of reference that are fixed with respect to the tank and fixed with respect to the fluid relate the current set-up to an oscillatory forcing of angular frequency

$$\omega = w_a m \tag{1}$$

that is fixed relative to the fluid.

Observations

The flow in all experiments evolved in a qualitatively similar manner. Once the forcing at the surface was ini-

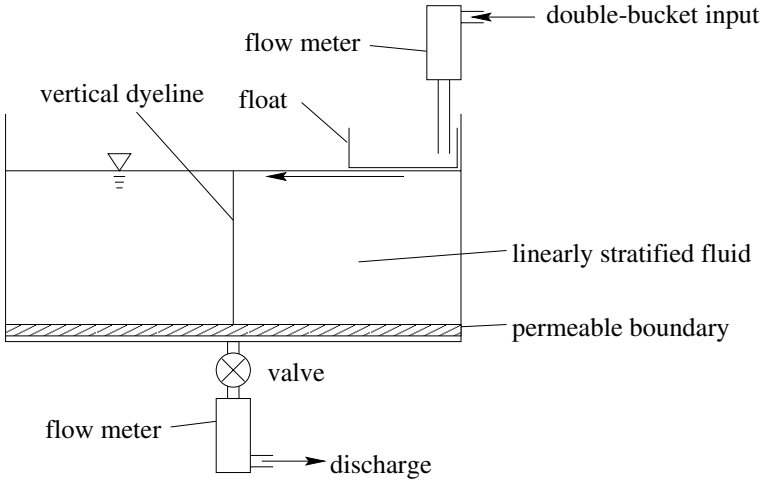

Figure 1: Side-on view of experimental set-up. The tank was 120 cm in length, 8 cm in width and filled so that the depth of fluid above the permeable boundary was 30 cm.

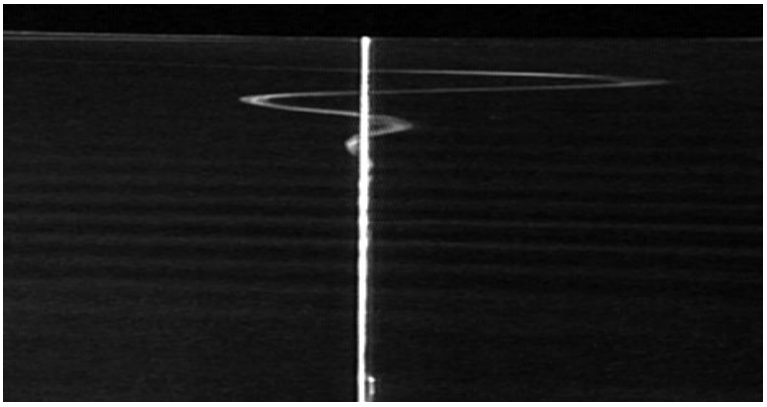

Figure 2: Visualisation of the horizontal velocity profile (side-on view of the tank) due to the steady-state internal wavefield generated by the forcing at the free surface. The free-surface can be seen close to the top of the photograph. Advection of the initially vertical dye line (superposed in white) has a short time later produced the oscillatory dye line (also shown in white) whose amplitude decays with depth. The field of view corresponds approximately to the full flow depth (30 cm) above the permeable boundary.

tiated, dye was observed to be advected strongly away from the float by the horizontal outflow. Internal waves radiated energy downwards from the surface forcing. A perturbation in the vertical dye line developed a short time later just below the outflow layer. This perturbation grew to form a second layer that flowed in the opposite direction to the outflow, i.e. towards the float. The continued transport of energy by the wavefield gave rise in turn to a series of alternately-signed perturbations in the dye line that decay with depth. These perturbations grew and formed a series of counterflowing layers, each weaker than the one above.

The internal wavefield reached a steady-state following the transient evolution just described. The subsequent release of vertical dyelines showed the horizontal velocity profile to maintain the same form, an example of which is shown in Figure 2.

Measurements of the steady-state internal wavefield are presented in Figure 3. The dimensionless vertical advection velocity w_a' is plotted as a function of the dimensionless vertical wavelength λ/H. The data points show a systematic dependence upon the Reynolds number Re. It is apparent that an increase in the vertical advection velocity w_a, while holding L' and Re constant, caused the vertical wavelength of the excited wave mode to increase. The ordinate in Figure 3 is equivalent to ω'/mH for oscillatory forcing at dimensionless frequency ω' in the frame of reference fixed with respect to the fluid. The rate of amplitude attenuation with height is observed in experiments to decrease as w_a increases.

Outline of theory

Wong *et al.* [3] observed a series of horizontal counterflowing layers (termed "shear layers") in a plume filling box experiment. They demonstrated that the shear layers correspond to internal gravity wave modes whose vertical phase velocity c_y is approximately equal and oppositely directed to the vertical advection velocity. I apply the same criteria to predict the vertical wavelength of internal wave modes in this experiment.

Consider first the inviscid dispersion relation for internal waves (e.g. see Lighthill [2]),

$$\omega' = \frac{k}{(k^2+m^2)^{1/2}}, \qquad (2)$$

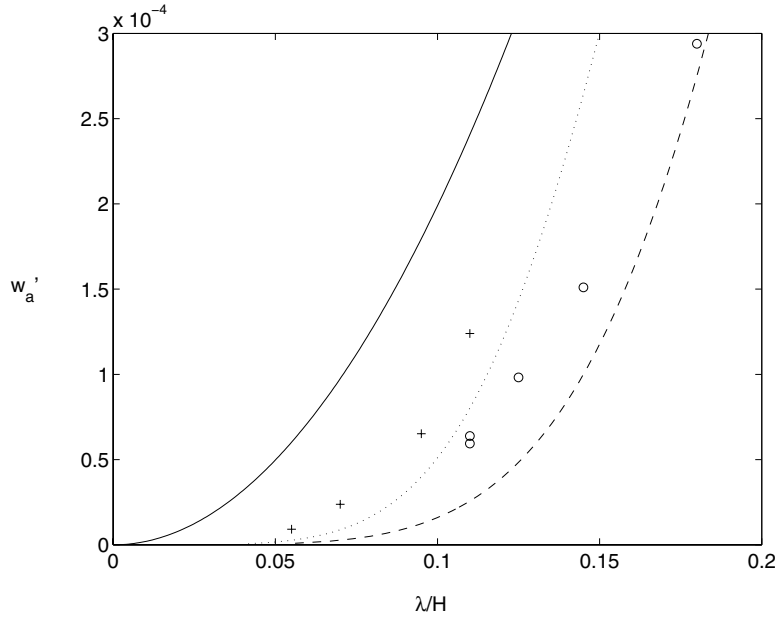

Figure 3: Comparison of theoretical predictions and experimental measurements for the dimensionless vertical advection velocity as a function of dimensionless vertical wavelength: —— inviscid theory; $Re = 3.5 \times 10^4, L' = 0.25$ - - - - theory, ∘ measurement; $Re = 11.5 \times 10^4, L' = 0.25$ ····· theory, + measurement.

where $\omega' = \omega/N$ is the dimensionless frequency. Assuming the density gradient to be constant and the vertical advection to be spatially uniform, the requirement that $c_y = w_a$ may be written as

$$mH = \left(\frac{\pi L'}{2}\right)^{1/2} \left[\left(\pi^2 L'^2 + \frac{4}{w_a'^2}\right)^{1/2} - \pi L'\right]^{1/2}. \quad (3)$$

The horizontal wavenumber k is chosen to be π/L, which corresponds to the lowest mode that gives zero horizontal velocity at the vertical tank boundaries. Equation (3) will be found to give dimensionless wavelengths $\lambda/H = 2\pi/mH$ that are significantly smaller than those observed in the w_a' regime of the current experiments.

Wong *et al.* [3] obtained the dispersion relation governing linear internal waves in a viscous non-diffusive fluid with uniform buoyancy frequency:

$$-\mathrm{i}\nu\omega\kappa^4 + \omega^2\kappa^2 - N^2k^2 = 0, \quad (4)$$

where $\kappa = (k^2 + m_\nu^2)^{1/2}$ is the total wavenumber of a travelling wave mode in a frame of reference that is fixed relative to the fluid and m_ν denotes the vertical wavenumber in the viscous fluid. The wavefield is assumed to be two-dimensional, with no variation across the tank width.

The general solution of equation (4) gives four complex roots for κ, but only one root is physically realisable. This root corresponds to wave modes that radiate energy away from the forcing while decaying in amplitude. The real part of the vertical wavenumber in this root may be expressed in dimensionless form (see [3]) as

$$\begin{aligned}\Re(m_\nu H) &= \frac{2\pi}{\lambda/H} \\ &= \frac{\sqrt{\omega' Re}}{2}\left[|X| - |\beta|\sin\left(\frac{\phi}{2}\right) - \frac{2\pi^2 L'^2}{\omega' Re}\right]^{1/2}, \quad (5)\end{aligned}$$

where

$$\begin{aligned}X &= \left[\left(|\beta|\cos\left(\frac{\phi}{2}\right) - 1\right)^2\right. \\ &+ \left.\left(|\beta|\sin\left(\frac{\phi}{2}\right) + \frac{2\pi^2 L'^2}{\omega' Re}\right)^2\right]^{1/2}, \quad (6)\end{aligned}$$

$$\tan\phi = -\frac{4\pi^2 L'^2}{\omega'^3 Re}, \qquad -\pi/2 < \phi \le 0, \quad (7)$$

and

$$|\beta| = \left[1 + \left(\frac{4\pi^2 L'^2}{\omega'^3 Re}\right)^2\right]^{1/4}. \quad (8)$$

The inviscid and viscous dispersion relations predicted by equations (3) and (5) are plotted in Figure 4 for several combinations of the parameters L' and Re. Viscously damped internal waves (dashed lines) show very different asymptotic behaviour at low frequency when compared with inviscid predictions (solid lines). This behaviour might be anticipated on physical grounds. Momentum transport in the vertical due to viscosity will increase at low frequency, thus acting to slow the natural frequency of oscillation compared with that in an inviscid fluid. The viscously damped regime is a strong function of flow aspect ratio L' and Reynolds number Re, but is typically important for values of ω' up to $O(10^{-2})$ or higher.

As the effects of viscous damping become relatively weaker the fluid motion, which is nearly horizontal at low frequencies, is expected to be coupled over a region of lesser vertical extent. Accordingly the breakpoint between inviscid and viscous behaviour in Figure 4 moves to lower frequency/higher wavenumber as Re increases (cf. curves 3 and 4 with curve 1).

When the flow aspect ratio is decreased both the inviscid and viscous dispersion relations are shifted to the left in

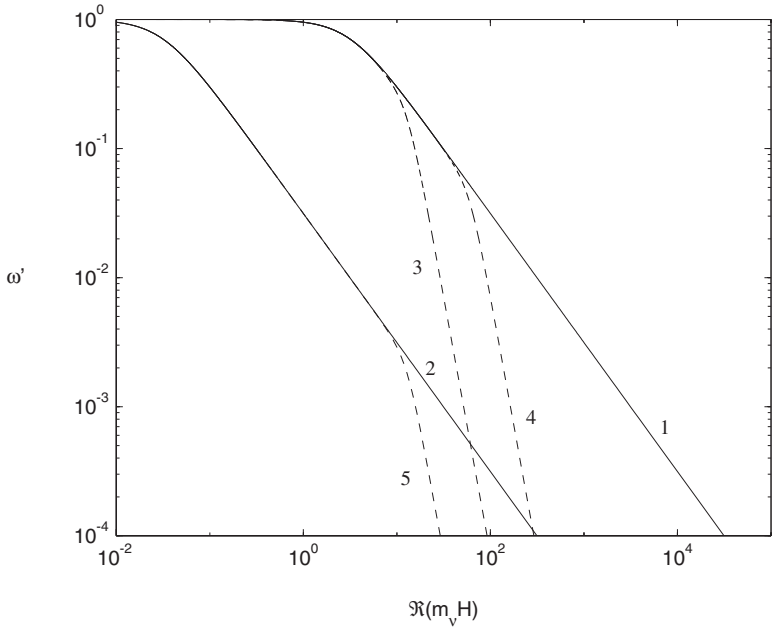

Figure 4: Comparison of dispersion relations from inviscid and viscous theory. Dimensionless frequency ω' is plotted as a function of the real part of the dimensionless vertical wavenumber $\Re(m_\nu H)$ for 1) $L' = 1$, inviscid; 2) $L' = 0.01$, inviscid; 3) $L' = 1, Re = 10^3$; 4) $L' = 1, Re = 10^5$ and 5) $L' = 0.01, Re = 10^5$.

Figure 4. This behaviour occurs because the wavelength of the assumed horizontal mode increases, i.e. the horizontal wavenumber $k = \pi/L$ decreases. Thus motion associated with a particular vertical wavenumber becomes closer to horizontal in the frame of reference fixed with the fluid and, by equation (2), the intrinsic frequency of oscillation decreases. If the relative strength of viscous damping is indicated by the range of frequencies in which inviscid and viscous behaviour coincides, it is surprising that viscous damping becomes relatively weaker as the flow aspect ratio decreases (cf. curves 4 and 5 with curves 1 and 2, respectively, in Figure 4). This behaviour is the topic of further investigation.

The predictions of inviscid and viscous theory with $L' = 0.25$ are also plotted in Figure 3 for direct comparison with experimental measurements. The solid curve corresponds to equation (3) while the dashed and dotted curves correspond to equation (5) with $Re = 3.5 \times 10^4$ and 11.5×10^4, respectively. As viscous damping becomes stronger (i.e. Re decreases) it is apparent that the wavelength of a given mode increases. This observation is consistent with stronger vertical coupling of the wave motion and with the decrease in natural oscillation frequency noted in the discussion above. The theory incorporating viscous damping provides much-improved predictions of the internal wavefield compared with traditional inviscid theory.

Conclusions

I have used both experiments and theory to examine the characteristics of damped internal waves in a density-stratified fluid. Damping is observed to modify the internal wavefield in two ways. First, the wave amplitude decays with distance from the forcing. Second, for sufficiently strong damping, the intrinsic frequency of wave motion is reduced compared with that in an inviscid fluid. The regime of strong damping exists for low frequency wave motion over a wide range of flow aspect ratios and Reynolds numbers. A theory that incorporates spatially uniform damping is in good agreement with the strongly-damped internal wavefield observed in experiments.

The damping in the current experiments is due to viscosity but the results have application to flows at much larger scales where the damping is most likely due to background turbulence. However, the timescales upon which I anticipate damping to be most important are likely to be comparable with the period of Earth's rotation. Consequently I will undertake further work to study the effect of damping on internal inertia-gravity waves.

Acknowledgements

I am grateful to P. Kim and T. Beasley for assistance with the experiments, and to R.W. Griffiths and R.C. Kerr for helpful discussions and comments.

References

[1] LeBlond, P.H., On the damping of internal gravity waves in a continuously stratified ocean, *J. Fluid Mech.*, **25**, 1966, 121–142.

[2] Lighthill, M.J., *Waves in fluids*, Cambridge University Press, 1978.

[3] Wong, A.B.D., Griffiths, R.W. and Hughes, G.O., Shear layers driven by turbulent plumes, *J. Fluid Mech.*, **434**, 2001, 209–244.